

Acoustic signature of a submarine hull

Author/Contributor:

Caresta, Mauro; Kessissoglou, Nicole

Publication details:

Proceedings of the 14th International Congress on Sound and Vibration, Cairns, Australia, 9-12 July 2007

Event details:

Fourteenth International Congress on Sound and Vibration (ICSV14)
Cairns, Australia

Publication Date:

2007

DOI:

<https://doi.org/10.26190/unsworks/367>

License:

<https://creativecommons.org/licenses/by-nc-nd/3.0/au/>

Link to license to see what you are allowed to do with this resource.

Downloaded from <http://hdl.handle.net/1959.4/37261> in <https://unsworks.unsw.edu.au> on 2023-03-30

ICSV14
Cairns • Australia
9-12 July, 2007



ACOUSTIC SIGNATURE OF A SUBMARINE HULL

Mauro Caresta and Nicole Kessissoglou

School of Mechanical and Manufacturing Engineering, University of New South Wales
Sydney, NSW 2052, Australia
m.caresta@student.unsw.edu.au

Abstract

A model to predict the acoustic signature of a submarine resulting from the radial vibration of the hull under axial excitation is presented. The simplified physical model of the submarine hull includes complicating effects such as the presence of bulkheads, end enclosures, ring stiffeners and fluid loading due to the interaction with the surrounding medium. Under an axial symmetric force, only the 'breathing' modes of the cylinder corresponding to the $n=0$ circumferential modes are excited. To show the sound radiation due to the higher order $n \geq 1$ modes, a point axial force acting at one end of the shell has been considered. At low frequencies, the structural wavenumbers are generally subsonic. However, due to the finite cylinder, the wavenumber spectrum is a convolution of the spectrum of an infinite structure and a window generating radiation by means of the presence of supersonic components. The effect of the bulkheads on the structural and acoustic responses of the hull is also presented.

1. INTRODUCTION

Cylindrical structures are widely used in many engineering applications, namely, aircraft fuselages, piping systems and shells of maritime vessels. Vibration generated in these structures can generate fatigue and significant noise levels. Hence the study of the dynamic behaviour of such structures is of great importance. Vibrational modes of a submerged hull are excited from the transmission of fluctuating forces through the shaft and thrust bearings due to the propeller rotating in an unsteady fluid. These low frequency vibration modes of the hull can result in a high level of radiated noise. The focus of this work is to investigate the structural and acoustic responses of a submarine hull under axial excitation. Previous work has concentrated on the $n=0$ axisymmetric breathing modes [1]. However in reality, the excitation of the hull from the propulsion system is not perfectly symmetric, resulting in excitation of both the $n=0$ breathing modes and higher order circumferential $n \geq 1$ modes. The $n \geq 1$ modes can be efficient sound radiators due to the nature of the structural waves being mainly flexural.

2. DYNAMIC MODELLING OF A SUBMERGED HULL

To describe the low frequency dynamic response of a submarine, the hull has been modelled as a thin walled finite cylindrical shell. Various influencing effects such as the presence of bulkheads, end enclosures, ring stiffeners and fluid loading due to the interaction with the surrounding medium

are included in the dynamic model. Many investigators (Love, Flügge, Timoshenko and others) have developed differential equations for a thin cylindrical shell that arise from small differences in the formulation of the strain-displacement relationship. These differential equations have been summarised by Leissa [2]. Whilst the simplest equations of motion are the Donnell-Mushtari, the Flügge equations are more accurate at low frequencies and have been used in this work. The equations of motion are given in terms of the axial u , circumferential v , and radial motion w . As shown in Fig. 1, u , v and w are the orthogonal components of displacement in the x , θ and z directions, respectively. a is the mean radius of the cylindrical shell and h is the shell thickness.

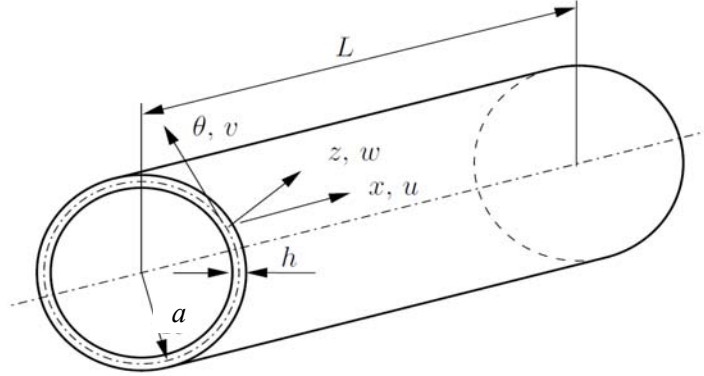


Figure 1. Coordinate system for a thin walled cylindrical shell.

In order to increase stiffness and strength and to reduce weight, the hull is reinforced with regularly spaced ring stiffeners. The effect of rings can be considered by averaging their properties over the surface of the shell. This method was originally derived by Baruch and Singer [3]. Ruotolo [4] showed that for stiffened cylinders, the Donnell-Mushtari can lead to very inaccurate results compared with the Flügge equations. The equations of motion for a stiffened cylindrical shell using the Flügge theory given by Rosen and Singer [5] have had extra terms added to take into account the fluid loading, internal structure and on-board equipment, and are given by the following

$$\frac{\partial^2 u}{\partial x^2} + \frac{q_1}{a^2} (1 + \beta^2) \frac{\partial^2 u}{\partial \theta^2} + \frac{q_2}{a} \frac{\partial^2 v}{\partial \theta \partial x} + \frac{v}{a} \frac{\partial w}{\partial x} - \beta^2 a \frac{\partial^3 w}{\partial x^3} + \beta^2 \frac{q_1}{a} \frac{\partial^3 w}{\partial x \partial \theta^2} - \frac{\gamma}{c^2} \frac{\partial^2 u}{\partial t^2} = 0 \quad (1)$$

$$\frac{q_2}{a} \frac{\partial^2 u}{\partial \theta \partial x} + d_1 \frac{\partial^2 v}{\partial \theta^2} + d_2 \frac{\partial^2 v}{\partial x^2} + d_3 \frac{\partial w}{\partial \theta} + d_4 \frac{\partial^3 w}{\partial \theta^3} - d_5 \frac{\partial^3 w}{\partial x^2 \partial \theta} - d \frac{\partial^2 v}{\partial t^2} = 0 \quad (2)$$

$$\frac{v}{a} \frac{\partial u}{\partial x} - \beta^2 a \frac{\partial^3 u}{\partial x^3} + \frac{\beta^2}{a} q_1 \frac{\partial^3 u}{\partial x \partial \theta^2} + d_3 \frac{\partial v}{\partial \theta} + d_4 \frac{\partial^3 v}{\partial \theta^3} - d_5 \frac{\partial^3 v}{\partial x^2 \partial \theta} + d_6 w + d_7 \frac{\partial^2 w}{\partial \theta^2} + \quad (3)$$

$$+ \beta^2 \left(d_8 w + d_9 \frac{\partial^2 w}{\partial \theta^2} + a^2 \frac{\partial^4 w}{\partial x^4} + d_{10} \frac{\partial^4 w}{\partial x^2 \partial \theta^2} + d_{11} \frac{\partial^4 w}{\partial \theta^4} \right) + d \frac{\partial^2 w}{\partial t^2} - \frac{p}{c^2 \rho h} = 0$$

where

$$\beta = \frac{h}{\sqrt{12a}}, \quad c = \sqrt{\frac{E}{\rho(1-\nu^2)}}, \quad q_1 = \frac{1-\nu}{2}, \quad q_2 = \frac{1+\nu}{2}, \quad \gamma = \left(1 + \frac{A}{bh} + \frac{m_{eq}}{\rho h} \right) \quad (4-8)$$

$$d = \frac{1}{c^2} \left(1 + \frac{A}{bh} + \frac{m_{eq}}{\rho h} \right), \quad d_1 = \frac{1 + \mu}{a^2}, \quad d_2 = q_1(1 + 3\beta^2), \quad d_3 = \frac{1 + \mu + \chi + \beta^2 \eta}{a^2} \quad (9-12)$$

$$d_4 = \frac{\chi + \beta^2 \eta}{a^2}, \quad d_5 = \beta^2 \frac{3 - \nu}{2}, \quad d_6 = \frac{1 + \mu + 2\chi}{a^2}, \quad d_7 = \frac{2\chi}{a^2} \quad (13-16)$$

$$d_8 = \frac{1 + 3\eta}{a^2}, \quad d_9 = \frac{2 + 4\eta}{a^2}, \quad d_{10} = 2 + \eta_t, \quad d_{11} = \frac{1 + \eta}{a^2}, \quad \mu = \frac{(1 - \nu^2)EA}{Ebh} \quad (17-21)$$

$$\chi = \frac{(1 - \nu^2)EAz}{Ebh}, \quad \eta = \frac{EI}{bD}, \quad \eta_t = \frac{GJ}{bD}, \quad D = \frac{Eh^3}{12(1 - \nu^2)}. \quad (22-25)$$

β is the thickness parameter, c is the longitudinal wave speed, E , ρ and ν are respectively the Young's modulus, density and Poisson's ratio. The ring stiffeners have cross sectional area A , b is the stiffener spacing and z is the distance between the shell mid-surface and the centroid of a ring. G is the shear modulus, I is the area moment of inertia of the stiffener about its centroid and J is the polar moment of inertia of the cross sectional area. In Eq. (3), p is the fluid loading acting normal to the cylindrical surface and can be expressed in terms of an acoustic impedance [6]

$$p(x, \theta) = \dot{w}(x, \theta)(r_f - j\omega m_f) \quad (26)$$

m_f and r_f are respectively the reactive and resistive components of the impedance that introduce mass-like and damping-like effects. Their values are obtained using a standing wave approximation [6]. In Eqs. (8) and (9) m_{eq} represents the equivalent distributed mass of the internal structure and on-board equipment. In addition, the main ballast tank and casing have been taken into account by adding distributed masses around the circumference at each end. The cylindrical hull is closed at both ends and separated into three compartments by means of bulkheads. A schematic diagram of the modelled hull is shown in Fig. 2.

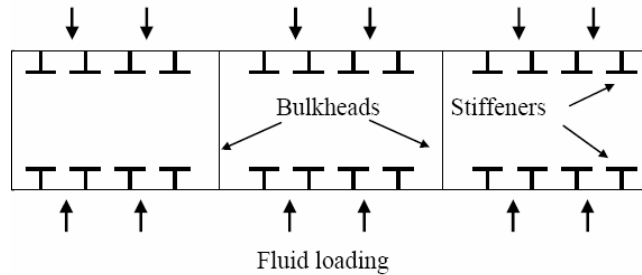


Figure 2. Schematic diagram of the hull.

The general solutions to the equations of motion given by Eqs. (1) to (3) can be written as [7]

$$u(x, \theta, t) = Ue^{jkx} \cos(n\theta)e^{-j\omega t}, \quad v(x, \theta, t) = Ve^{jkx} \sin(n\theta)e^{-j\omega t}$$

$$w(x, \theta, t) = We^{jkx} \cos(n\theta)e^{-j\omega t} \quad (27-29)$$

These solutions represent a wave travelling in the axial direction and standing with n nodal lines in the circumferential direction. k is the axial wavenumber. Substituting the general solutions into the differential equations of motion results in a dispersion equation in k and ω . For each value of k , the dispersion equation gives three different natural frequencies associated with flexural, extensional or torsional waves, which in turn are called waves of first, second and third class, respectively [8]. The smallest frequency represents primarily radial motion and the two other roots represent either primarily longitudinal or circumferential motion. However, at low frequencies, it is difficult to distinguish between the wave types because the vibrational behaviour of the shell becomes complex due to increased curvature of the wall relative to the wavelength of the shell. An exception is given by the $n=0$ mode, where the lowest frequency represents primarily axial motion.

Substituting the general solutions given by Eqs. (27) to (29) into the equations of motion results in three linear equations in terms of U , V and W , that can be arranged in matrix form as $\mathbf{A}\mathbf{u} = \mathbf{0}$, where $\mathbf{u} = [U \ V \ W]^T$ contains the unknown wave amplitudes and T is the transpose. For a non-trivial solution, the determinant of the matrix \mathbf{A} must be zero. The expanded determinant results in an eighth order equation in k . Since the characteristic equation is a function of the fluid loading parameters m_f and r_f whose values depend on k , a numerical solution is required to determine the axial wavenumbers. For each value of k_i ($i=1$ to 8), the axial and circumferential amplitude ratios can be obtained as $C_i = U_i / W_i$ and $G_i = V_i / W_i$, respectively. For harmonic motion, the complete solutions are given by

$$u = \sum_{n=0}^{\infty} \sum_{i=1}^8 C_{n,i} e^{jk_{n,i}x} \cos(n\theta) e^{-j\omega t} \quad v = \sum_{n=0}^{\infty} \sum_{i=1}^8 G_{n,i} W_i e^{jk_{n,i}x} \cos(n\theta) e^{-j\omega t}$$

$$w = \sum_{n=0}^{\infty} \sum_{i=1}^8 W_{n,i} e^{jk_{n,i}x} \cos(n\theta) e^{-j\omega t} \quad (30-32)$$

The bulkheads and end enclosures have been modelled as thin plates with bending and in-plane motion. The equations of motion are given in ref. [7] and the general solutions for the bending w_p and in-plane, u_p and v_p , motions can be written as

$$w_p = \sum_{n=0}^{\infty} (A_{1n} J_n(k_{pB}a) + A_{2n} I_n(k_{pB}a)) \cos(n\theta) e^{-j\omega t} \quad (33)$$

$$u_p = \sum_{n=0}^{\infty} (B_{1n} \partial J_n(k_{pL}a) / \partial a + n B_{2n} J_n(k_{pT}a) / a) \cos(n\theta) e^{-j\omega t} \quad (34)$$

$$v_p = - \sum_{n=0}^{\infty} (n B_{1n} J_n(k_{pL}a) / a + B_{2n} \partial J_n(k_{pT}a) / \partial a) \sin(n\theta) e^{-j\omega t} \quad (35)$$

k_{pL} is the plate bending wavenumber and k_{pT} , k_{pB} are the wavenumbers for in-plane, waves in the plate [7]. J_n , I_n are respectively Bessel functions and modified Bessel functions of the first kind. The dynamic response of the hull is expressed in terms A_j and B_j ($j=1, 2$ for each plate) and W_i ($i=1$ to 8 for each section of the hull) for a total of 40 unknown coefficients. The continuity/equilibrium equations at the shell and plate junctions leads to 40 equations that can be arranged in matrix form $\mathbf{B}\mathbf{X} = \mathbf{F}$, with \mathbf{X} the vector of unknown coefficients and \mathbf{F} is a vector

containing external forces. For given external forces, the wave amplitudes for each value of n can be found by $\mathbf{X} = \mathbf{B}^{-1}\mathbf{F}$.

3. RESULTS OF THE STRUCTURAL RESPONSE

Numerical calculations were performed on a ring stiffened steel cylinder of 3.25 m radius, 40 mm hull plate thickness, 45 m length, and with two evenly spaced bulkheads of thickness 40 mm. The stiffeners have a rectangular cross-section of base 80 mm and height 150 mm, and are separated by 0.5 m. The cylinder was submerged in water of density 1000 kg/m³. A neutrally buoyant condition was maintained by using distributed masses of 100 tonnes at each end while a distributed mass of 1000 kg/m² on the shell was used to take into account the on-board machinery. Internal structural damping was included in the analysis by using a structural loss factor of 0.02. The shell was axially excited by an external point force $F(x, \theta, t) = F_0 \delta(x) \delta(\theta) e^{-j\omega t}$ on one end of the cylindrical shell, where a unity force amplitude ($F_0 = 1$) has been used. Figures 3 and 4 respectively represent the frequency response function (FRF) of the axial and radial displacements at the drive point location ($x=0$). In each figure, the FRF for the $n=0$ breathing modes and including the higher order modes are shown. In both figures, it is evident that the higher order modes, in particular the $n=1$ bending modes, significantly contribute to the low frequency structural responses. From the FRF of the radial displacement, it is evident the necessity to consider the $n \geq 1$ modes as their flexural influence is strong and thus greatly contribute to the sound radiation. At low frequencies, modes corresponding to $n \geq 3$ are negligible.

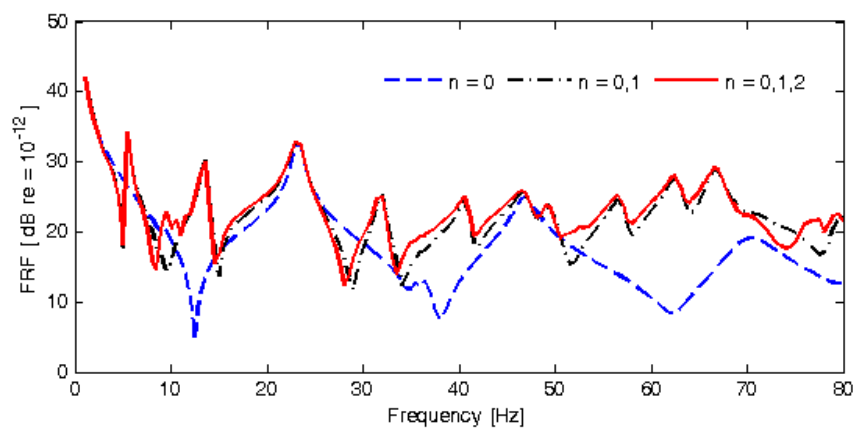


Figure 3. Frequency response function of the hull axial displacement at $x=0$.

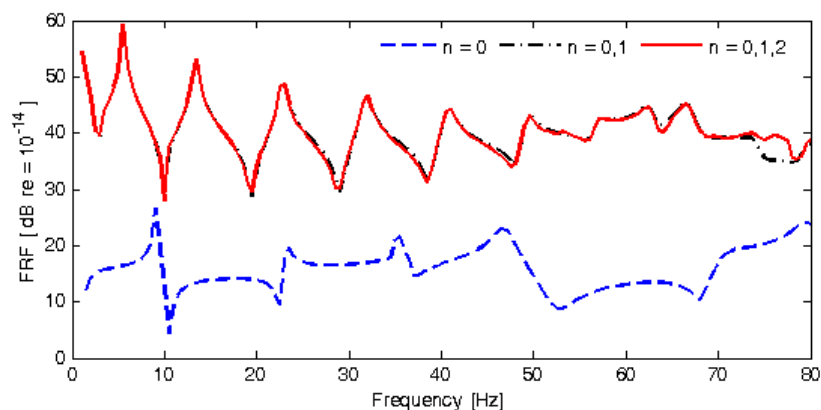


Figure 4. Frequency response function of the hull radial displacement at $x=0$.

4. SOUND RADIATION MODEL OF THE SUBMARINE HULL

The sound pressure in the far-field due to the radial motion of the hull is given by [6]

$$p(r, \theta, \varphi) = \frac{\rho_f e^{jk_f r}}{\pi k_f r \sin \theta} \sum_n \frac{\hat{w}(k_f \cos \theta) (-j)^{n+1}}{H'_n(k_f r \sin \theta)} \cos(n\varphi) \quad (36)$$

\hat{w} is the spatial Fourier transform of the radial acceleration. ρ_f is the density of the fluid, k_f is the acoustic wavenumber and H'_n is the derivative of the Hankel function of order n . Definition of the angles φ and θ are shown in Fig.5.

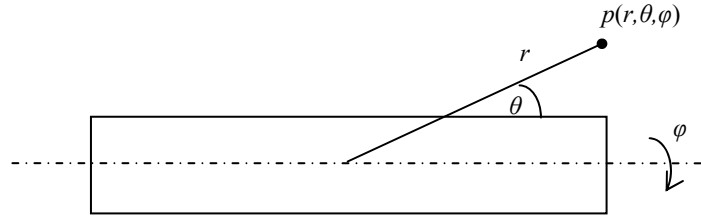


Figure 5. Definition of coordinate system for the field point.

An acoustic transfer function for each value of φ is defined as $H_s(r, \varphi) = \frac{\max_{0 \leq \theta \leq 2\pi} p(r, \varphi)}{F}$ where F is the axial point force applied at one end of the shell described previously. Figure 6 shows the FRF of the acoustic transfer function, again for the $n=0$ modes and including the higher order modes. The strong influence of the $n=1$ modes is clearly shown while the $n=2$ modes fall in the subsonic region and thus are not efficient sound radiators.

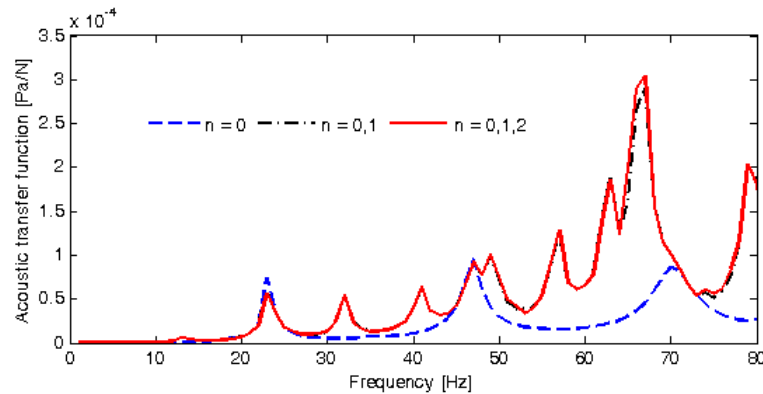


Figure 6. Frequency response of the acoustic transfer function at $r = 1000$ m and $\varphi = 0$.

The spatial Fourier transform of the radial velocity shows the effect of the finite structure contributing to the radiated sound pressure. Discontinuities associated with the finite cylinder ends have resulted in a scattering of the energy from subsonic to supersonic wavenumber components [9]. Figure 7 shows the radial velocity level of the hull as a function of the structural wavenumber at the resonant frequency of 67 Hz. For a speed of sound for water of 1500 m/s, the corresponding acoustic wavenumber is 0.28 m^{-1} . As observed in Fig. 6, this frequency corresponds to a very high peak in the acoustic response which is attributed to the $n=1$ mode. Comparison of the magnitudes

in Fig. 7 shows that the supersonic wavenumber components for the $n=1$ modes in the supersonic region ($k < k_f$) are significant and thus correspond to radiating wavenumber components.

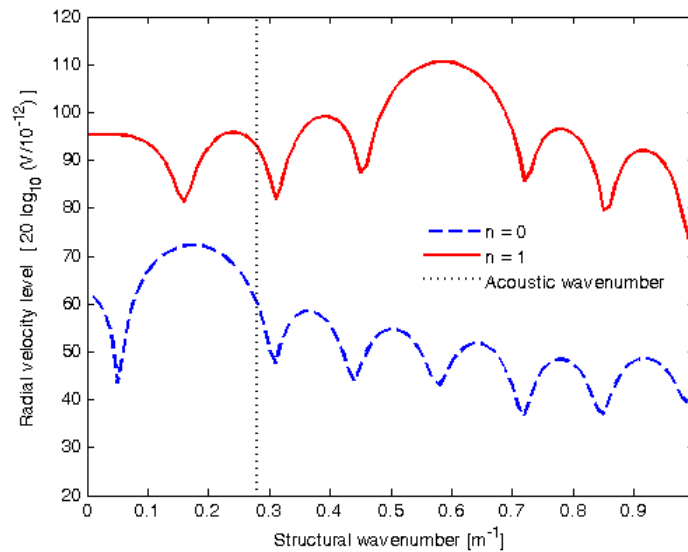


Figure 7. Radial velocity spectrum at 67 Hz for the $n=0$ and $n=1$ modes.

5. EFFECT OF THE BULKHEADS ON THE HULL RESPONSES

It is interesting to focus on the effect of the bulkheads on the structural and acoustic responses of the hull. In Fig. 8 it can be observed that the bulkheads create a phenomenon of grouping for the $n=2$ modes, while the resonant frequencies of the breathing and bending modes are the same as before.

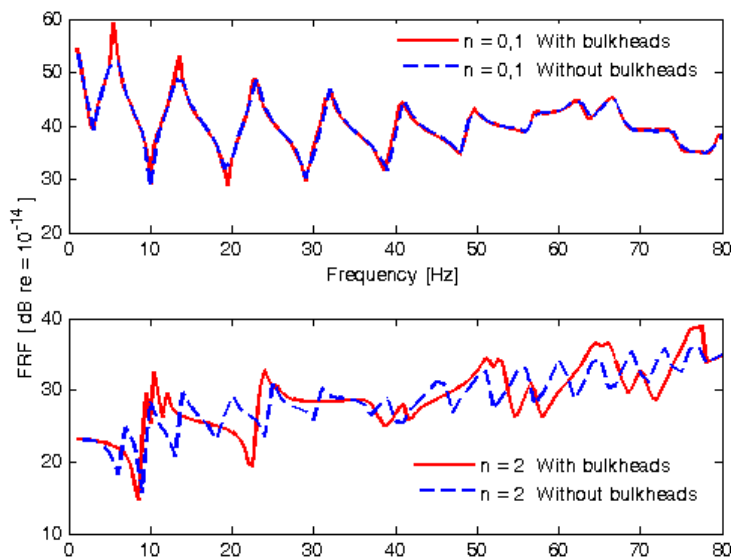


Figure 8. Frequency response function of the hull radial displacement at $x=0$.

Figure 9 shows the sound radiation with and without the bulkheads. As expected, the radiated sound pressures in both cases are nearly the same. This is because the presence of the bulkheads affects only the $n \geq 2$ modes that are not efficient sources of sound (as discussed in Fig. 6).

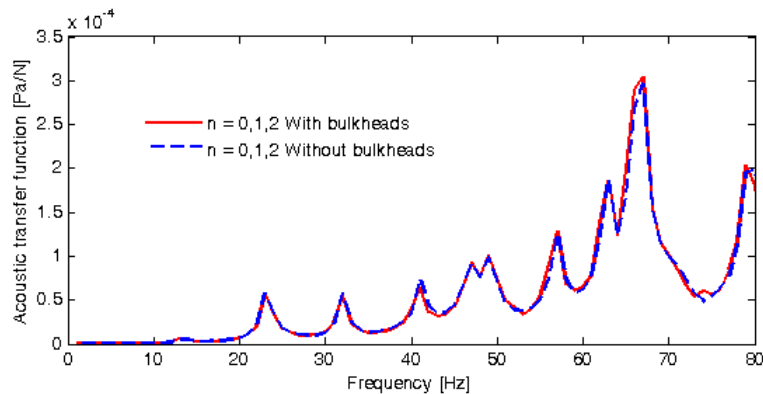


Figure 9. Frequency response of the acoustic transfer function at $r = 1000$ m and $\varphi = 0$.

6. CONCLUSIONS

A model to describe the dynamic behaviour of a submarine hull with several complicating effects such ring stiffeners, bulkheads, end enclosures and fluid loading, under axial excitation has been developed. The sound radiation due to the radial motion of the hull has been presented. Results show that it is necessary to include higher order circumferential modes at low frequencies in order to obtain the total radiated sound pressure of the hull. The effect of the bulkheads on the structural and acoustic responses of the hull has also been presented, showing influence on modes of order $n=2$.

REFERENCES

- [1] Y. Tso, N.J. Kessissoglou and C. Norwood, "Active control of a fluid-loaded cylindrical shell, part 1: dynamics of the physical system", *Proceedings of the Eighth Western Pacific Acoustics Conference (Wespac8)*, 7-9 April 2003, Melbourne, Australia.
- [2] A.W. Leissa, *Vibration of shells*, American Institute of Physics, Woodbury, New York, 1993.
- [3] M. Baruch and J. Singer, "Effect of eccentricity of stiffeners on the general instability of stiffened cylindrical shells under hydrostatic pressure", *Journal of Mechanical Engineering Science* **35**, 23-27 (1963).
- [4] R. Ruotolo, "A comparison of some thin shell theories used for the dynamic analysis of stiffened cylinders", *Journal of Sound and Vibration* **243**, 847-860 (2001).
- [5] A. Rosen and J. Singer, "Vibrations of axially loaded stiffened cylindrical shells", *Journal of Sound and Vibration* **34**, 357-378 (1974).
- [6] M.C. Junger and D. Feit, *Sound, structures and their interaction*, MIT Press, 1985.
- [7] Y.K. Tso and C.H. Hansen, "Wave propagation through cylinder/plate junctions", *Journal of Sound and Vibration* **186**, 447-461 (1995).
- [8] P.W. Smith, "Phase velocities and displacements characteristics of free waves in a thin cylindrical shell", *Journal of the Acoustical Society of America* **27**, 1065-1072 (1955).
- [9] C.R. Fuller, S.J. Elliott and P.A. Nelson, *Active control of vibration*, Academic Press, London, 1996.